

HOSTED BY



Contents lists available at ScienceDirect

Journal of King Saud University – Science

journal homepage: www.sciencedirect.com

Original article

S-adenosylmethionine synthase-derived GR15 peptide suppresses proliferation of breast cancer cells by upregulating the caspase-mediated apoptotic pathway: *In vitro* and *in silico* analyses



Manikandan Velayutham^a, B. Haridevamuthu^a, Mohamed Farouk Elsadek^b, Humaira Rizwana^c, Annie Juliet^d, Kanchana M. Karuppiyah^{e,*}, Jesu Arockiaraj^{a,*}

^a Department of Biotechnology, College of Science and Humanities, SRM Institute of Science and Technology, Kattankulathur 603 203, Chennai, Tamil Nadu, India

^b Department of Community Health Sciences, College of Applied Medical Sciences, King Saud University, Riyadh 11451, Saudi Arabia

^c Department of Botany and Microbiology, College of Science, King Saud University, P.O. Box 11495, Riyadh, Saudi Arabia

^d Institute for Cellular and Molecular Biology, The University of Texas at Austin, University Station A4800, Austin, TX 78712, USA

^e Department of Medical Research, Medical College Hospital and Research Centre, SRM Institute of Science and Technology, Kattankulathur, 603 203 Chennai, Tamil Nadu, India

ARTICLE INFO

Article history:

Received 11 July 2022

Revised 29 September 2022

Accepted 29 September 2022

Available online 6 October 2022

Keywords:

S-adenosylmethionine synthase

Spirulina

Oxidative stress

Antioxidant

Toxicity

ABSTRACT

Introduction: GR15 peptide is a potential antioxidant peptide which reduces intercellular ROS levels in zebrafish larvae stressed with H₂O₂. Cancer is a condition which develops during oxidative stress due to various reasons. Antioxidant molecules promote apoptosis or inhibit cancer cell proliferation by regulating the ROS level in cancer cells. This study identifies the anti-cancer potency of GR15 peptide derived from S-adenosylmethionine synthase of spirulina, *Arthrospira platensis*. We examined the anti-cancer property of this antioxidant peptide against breast cancer cells, MCF-7.

Methods: An *in-vitro* anticancer activity of GR15 peptide was investigated by performing the following assays: MTT, Trypan blue assay, LDH assay and IC50 value calculation. Moreover, we examined the morphology of cancer cells under inverted microscope due to apoptosis staining AO/PI. The inter-cellular cancer level was measured by DCFDA staining, and the mitochondrial membrane potential was determined by Rhodamine 123. Further, the FACS analysis was performed to identify the changes in the cell cycle phases. Altered mRNA expressions of anti-cancer genes including Bcl-2, BAX, Caspase 3 and Caspase 9 were also addressed.

Results: The GR15 peptide exhibit dose-dependent activity on MCF-7 cells. The MTT assay revealed that the GR15 peptide treatment at 45 μM showed 57 % inhibition of cancer cell proliferation. Also, the peptide significantly affects the cellular morphology and promotes apoptosis. GR15 treatment reduces the ROS level in a dose-dependent manner. The peptide is also exhibited mitochondrial membrane potential activity. As GR15 significantly upregulated the anti-cancer gene expression, an *in-silico* analysis was carried out to validate the anti-cancer activity. The molecular docking of GR15 showed good binding scores and significant amino acid interaction with the respective receptors.

Conclusion: This study suggested that GR15 potentiates anticancer activity. It reduces ROS and subsequently regulates caspase-mediated apoptosis. Overall, the observations suggested that GR15 could be an anti-cancer peptide; however, further studies on *in-vivo* mammalian model or clinical trials need to be performed to prove the claims.

© 2022 The Author(s). Published by Elsevier B.V. on behalf of King Saud University. This is an open access article under the CC BY-NC-ND license (<http://creativecommons.org/licenses/by-nc-nd/4.0/>).

* Corresponding authors.

E-mail addresses: kanchank1@srmist.edu.in (K.M. Karuppiyah), jesuaroa@srmist.edu.in (J. Arockiaraj).

Peer review under responsibility of King Saud University.



1. Introduction

Cancer is a heterogeneous disease defined by uncontrolled cell proliferation that can spread to other body parts. It is an intricate disease that causes serious clinical challenges; also it causes the deaths of millions of people worldwide, and it has been the subject of extensive research for both pathogenesis and therapeutics (Correia et al., 2021). The Cancer Research Center in the UK

<https://doi.org/10.1016/j.jksus.2022.102354>

1018-3647/© 2022 The Author(s). Published by Elsevier B.V. on behalf of King Saud University.

This is an open access article under the CC BY-NC-ND license (<http://creativecommons.org/licenses/by-nc-nd/4.0/>).

reported that the cancer rate will reach about 62 % in 2040 (Mikaelian et al., 2020). Cancer is the second leading risk factor for death in 183 countries, according to the World Health Organization (WHO) (Bray et al., 2021; Sung et al., 2021). Breast cancer has been the most commonly diagnosed cancer among women (Sung et al., 2021). Breast cancer is divided into progesterone, estrogen, and human epidermal receptor 2 (HER2) subgroups. The most dangerous form of breast cancer is triple-negative breast cancer because, this form lacks all the receptors that are commonly seen in breast cancer (Anjum et al., 2017). Despite significant progress in cancer research, breast cancer remains a critical healthcare issue (Anastasiadi et al., 2017). In recent years, peptide-based therapeutics for cancer treatment has gained attention. anti-cancer property of the peptides was achieved by targeting the cancer cells through various biological mechanisms such as inhibition of angiogenesis, regulation of apoptotic gene expression and targeting the signal transduction pathways (Kurrikoff et al., 2019).

Microalgae are a rich source of high-quality protein products such as protein concentrates, protein hydrolysates, and peptides; these products have several biological functions including antimicrobial, antioxidant, anti-inflammatory, and anti-cancer effect (Guzmán et al., 2019). Antioxidant agents restrict the proliferation of cancer cells by decreasing the level of reactive oxygen species (ROS) in cancer cells (Fleischauer et al., 2003). Several antioxidant molecules developed from *Arthrospira platensis* have been reported for their anti-cancer effects. According to previous reports *A. Platensis* is a rich source of peptides with varied bioactivity (Silva et al., 2021), yet, several biological functions of new and existing peptides remain unexplored.

The antioxidant peptide, GR15 has been previously developed from the protein sequence, S-adenosylmethionine synthase of *A. platensis*, the physicochemical properties of the GR15 peptide matches with the antioxidant requirement, which has been established, *in-vitro* and *in-vivo* earlier (Velayutham et al., 2021). Based on this observation, we hypothesize that the GR15 peptide have anti-cancer effect due to its antioxidant potential. This study has investigated the *in-vitro* anti-cancer potential of GR15 peptide on breast cancer cells, MCF-7.

2. Materials and methods

2.1. Maintenance of cell culture

The breast cancer cells, MCF-7, were obtained from the Department of Virology, The King Institute of Preventive Medicine and Research, Guindy, Chennai, India. Cells were cultured and maintained in a 5 % CO₂ incubator at 37 °C. The cells were grown in DMEM high glucose (4.5 g/L) supplemented with 10 % (FBS Gibco, Sydney, Australia), and 1 % antibiotics (10,000 U/L of penicillin/streptomycin).

2.2. In-vitro anti-cancer activity of GR15 against MCF-7 cells

The anti-cancer potency of the GR15 was determined by accessing the anti-proliferative and growth inhibition activity through the MTT assay. In brief, MCF-7 cells were seeded at a density of 1x10⁶ cells/0.2 mL/well in 96-well plates. Cells were treated with GR15 at doses of 5, 15, 25, 35, and 45 µM for 24, 48, and 72 h after achieving the optimum confluency. Untreated cells were used as the control. A 10 µl MTT solution (5 mg/mL of 3-(4,5-dimethylthiazol-2-yl)-2,5-diphenyl tetrazolium bromide) was added and incubated in the dark for 4 h. Finally, 100 µl of dimethyl sulphoxide was used to dissolve the formazan crystals. In an ELISA reader, absorbance was measured at 570 nm. Percentage inhibition was calculated using the formula below (Velayutham et al., 2022b).

$$\text{Percentage of inhibition} = \left[\frac{\text{Absorbance of control cells} - \text{Absorbance of treated cells}}{\text{Absorbance of control cells}} \right] \times 100\%$$

GraphPad Prism software calculated the effective anti-cancer activity by computing the IC₅₀ value (the concentration that induced 50 % cell death) of the data acquired from the inhibition rate.

2.3. Trypan blue assay

Percentage of dead and viable cells was calculated to determine the anti-cancer effect. Trypan blue exclusion assay was performed as described by Chiu et al. (Chiu et al., 2016).

2.4. Lactose dehydrogenase release assay

Cytotoxic effect of GR15 was determined by measuring the LDH levels as described by Crupi et al. (2020) with minor modifications. In brief, MCF-7 cells were treated as described previously (in section 2.2.1). Concentrations of LDH were measured as LDH inside the cell (LDH in), and LDH released in the medium (LDH out). Two samples i.e., cell homogenate and culture medium were collected at the end of the treatment period. A 50 µl sample was mixed with the 2 mL of the reaction mixture, NADH (0.20 mmol dm⁻³) and Tris buffer (61.43 mmol dm⁻³) (pH, 7.4) and incubated for 15 min. Then, 200 µl of pyruvate (21.5 mmol dm⁻³) was added, and the absorbance was measured at 339 nm in an ELISA reader. The following formula calculated the total LDH release (Al-Qubaisi et al., 2011).

$$\%LDH = \left(\frac{LDH_{out}}{LDH_{out} + LDH_{in}} \right) \times 100\%$$

2.5. Effect of GR15 peptide on cell morphology

To determine whether or not GR15 influences the MCF-7 cellular morphology. Abnormalities in the cellular morphology were evaluated under a phase-contrast inverted microscope at a magnification of 20X, and photographs were recorded (Prabha et al., 2020).

2.6. Analysis of apoptosis

The potency of GR15 to induce apoptosis was identified using a fluorescent staining assay according to previous protocol (Velayutham et al., 2022b). In brief, cells were treated as mentioned in section 2.3.1. Cells exposed to GR15 were stained with 100 µg/mL acridine orange and 100 µg/mL propidium iodide (AO/PI ratio of 1:1) for 30 min. Cells were observed under the fluorescence microscope at 20X magnification, and the results were recorded as photomicrographs.

2.7. Intracellular ROS level analysis

The DCFDA (2,7-dichlorodihydrofluorescein diacetate) staining assay was performed as described previously (Velayutham et al., 2022b).

2.8. Mitochondrial membrane potential assay

The mitochondrial membrane potential of GR15 was determined, as described by Ahamed and Alhadlaq (2014), with minor modifications. In brief, cells were treated as mentioned in section 2.3.1. The treated cells were stained with rhodamine 123 dye at a concentration of 10 µg/mL for 30 min in the dark. Excess stain

was removed by PBS washing, and the results were recorded as images observed under the fluorescence microscope at 20X magnification. Fluorescent intensity was measured by processing the images in ImageJ software (V.1.49, NIH, USA).

2.9. FACS analysis

Cells were treated with 25 or 45 μM of GR15 for 24 h at room temperature, while the untreated cells remained as the control. Fluorescent activated cell sorting analysis was carried out as described (Velayutham et al., 2022). In brief, the cells were fixed by overnight ice-cold ethanol treatment at -20 °C. Then, the cells were stained with 10 μl of propidium iodide (1 mg/ml) for 20 min after washing with 20 μl RNase (0.1 mg/ml) and 0.5 % Triton X-100. Samples were processed in the flow cytometer, and the Cell Quest Software (Becton Dickinson, USA) was used to analyze the data.

2.10. anti-cancer gene expression analysis

MCF-7 cells were treated with 25 or 45 μM of GR15 peptide for 24 h at room temperature. Untreated cells remained as control. Both the treated and untreated cells were considered for qRT-PCR assay. For the assay, we followed the standardized protocol; also, the thermal profile (Velayutham et al., 2022). List of primers utilized for the anti-cancer gene expression study are listed in Table 1 (Al-Harbi et al., 2020).

2.11. Molecular docking

Molecular docking analysis was carried out to validate the *in-vitro* observations, i.e., the anti-cancer effect of GR15. The HPEP-DOCK web server was used to perform the docking assay. We obtained free access to the webserver at <https://huanglab.phys.hust.edu.cn/hpepdock/> (Çakır et al., 2021). The PDB structures of anti-cancer proteins were obtained from the RCSB PDB Protein Data Bank (<http://www.rcsb.org/pdb/home/home.do>) (Chen et al., 2019). Anticancer proteins were used as receptors for docking, which includes Bcl-2 (PDB ID: 2XA0) (Chen et al., 2019), Bax (Pdb:1F16) (Zarei et al., 2020), caspase-3 (PDB ID: 1RHM) and caspase-9 (PDB ID: 3IBF) (Velayutham et al., 2022). Docking results were visualized in the discovery studio software.

2.12. Statistical study

Data represents an average of three replicates along with standard deviation (SD). The significant level of the obtained data was estimated in one-way ANOVA and post-ANOVA, Tukey's Multiple Range Test using the statistical package Graph Pad Prism (Ver.5.0).

3. Results

3.1. Anti-proliferative effect of GR15 on MCF-7 cells

In MCF-7 cells, MTT assay shows that GR15 challenge inhibits cell proliferation in a concentration-dependent manner. The lowest

concentration, 5 μM, inhibited to about 12 %, and the highest concentration, 45 μM, showed 57 % inhibition at 24 h treatment. Similarly, at 48 h challenge, 5 μM inhibited to about 19 %, and 45 μM showed 67 % inhibition. There was a reduction in the inhibitory effect at 72 h treatment, wherein the inhibition was 21 % in 5 μM, 59 % in 35 μM, and 57 % in 45 μM. These observations show that the inhibitory effect is concentration-dependent, but not time-dependent (Fig. 1). The IC50 values of GR15 were calculated based on the percentage of inhibition, obtained from the MTT assay. The IC50 values are 27.6 μM for 24 h, 29 μM for 48 h, and 31 μM for 72 h.

The number of live and dead cell percentages was calculated by the conventional cell count method, trypan blue staining assay. There was a dose-dependent increment in the dead cell percentage and a decrease in the live-cell percentage (E-Suppl. Fig. 1). The cellular membrane disruption potential of GR15 was investigated by LDH assay (Fig. 2), which showed a concentration-based increase in the percentage of LDH released at 24 h, 48 h, and 72 h, when compared with the control.

3.2. Effect of GR15 on cellular morphology and apoptotic induction

As the GR15 challenge inhibited the proliferation of MCF-7 cells, whether or not the peptide can influence the cellular morphology was also examined. Results revealed that 24 h treatment of GR15 affects the cellular morphology in a dose-dependent manner. The standard apoptotic characteristics, including the loss of cell rigidity, detachment from the bottom of the culture flask, and granulation shrinkage were observed (Fig. 3). The abnormal morphology in the peptide-treated cells was compared with the untreated control.

Acridine orange and propidium iodide staining showed that at the end of 24 h, in the five concentrations of GR15-treated MCF-7 cells apoptosis was induced (Fig. 4). Various stages of apoptosis, such as early apoptosis (fluorescent in yellow color), late apoptosis (fluorescent reddish-orange color), and necrotic cell death (reddish-brown color in fluorescent) were observed, on comparison with the untreated control. Viable cells were noticed in green color in the fluorescent field.

3.3. Intracellular reactive oxygen species level on MCF-7 cells

The effect of GR15 on the concentration of intracellular ROS was investigated through the DFCDA fluorescent staining. The untreated control cells showed higher fluorescent intensity than the GR15 treated cells. In the GR15 treated groups (five concentrations), there was a dose-dependent decrease in the fluorescent intensity, indicating that GR15 significantly reduced the ROS level in cancer cells (Fig. 5). Fluorescent intensity was quantified by ImageJ software (E-Suppl. Fig. 2). The untreated control showed a significantly higher fluorescent intensity of 82 %, whereas the GR15 treated groups exhibited a reduction in the intensities than the control, which are 77 %, 69 %, 50 %, 35 % and 30 % at 5 μM, 15 μM, 25 μM, 35 μM, and 45 μM, respectively. This observation identifies the significant dose-dependent effect of GR15 on ROS levels in MCF-7 cells.

Table 1
Primers used for the anti-cancer gene expression study.

Gene	Forward (5'-3')	Reverse (5'-3')
Bcl-2	GTGGATGACTGAGTACCT	CCAGGAGAAATCAACAGAG
BAX	TCAGGATGCGTCCACCAAGAAG	TGTGTCCACGGCGGAATCATC
Caspase-3	ACATGGAAAGCGAATCAATGGACTC	AAGGACTCAAATCTGTGGCCACC
Caspase-9	GCTCTTCCTTTGTTTCATC	CTCTTCCTCCACTGTTCAC
GAPDH (internal control)	GTCTCTCTGACTTCAACAGCG	ACCACCCTGTGCTGTAGCCAA

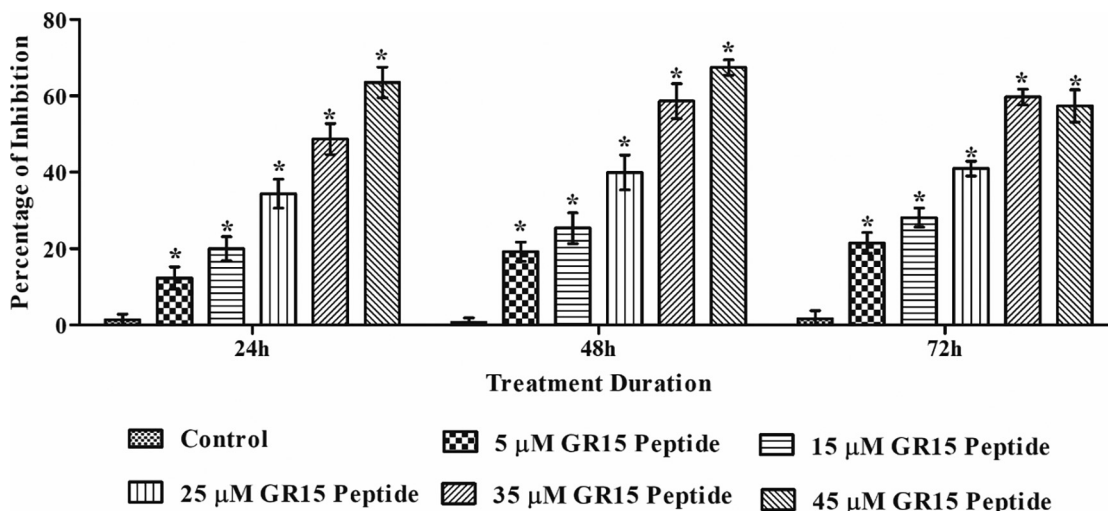


Fig. 1. Assessment of GR15 peptide antiproliferative activity in MCF-7 (Brest cancer cells) by MTT assay at various time intervals. The results were compared with the control (untreated) group, and the statistical significance ($p < 0.05$) is presented in asterisk (*). Data were presented in mean \pm standard deviation (SD) of three independent experiments.

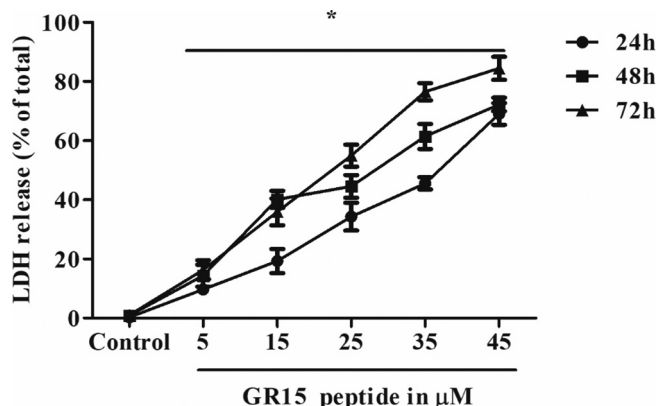


Fig. 2. Effect of GR15 peptide membrane disruption in MCF-7 cells assessed by total LDH leakage estimation. The data of the GR15 peptide-treated group was compared with the control (Untreated) group and showed a statistical significance at $p < 0.05$, indicated by the asterisk (*). Data expressed in mean \pm SD of three independent experiments.

3.4. Fluorescent microscopic analysis of mitochondrial membrane potential

The mitochondrial membrane potential of GR15 was analyzed using Rhodamine 123 fluorescent staining. The results revealed that GR15 functions on dose-dependent basis on the mitochondrial membrane potential activity (Fig. 6). The fluorescent effect was further quantified using ImageJ program (E-Suppl. Fig. 3). The untreated control (80 %) showed significantly higher fluorescent intensity than the GR15 treated cells as 71 % (5 μM), 63 % (15 μM), 67 % (25 μM), 45 % (35 μM) and 33 % (45 μM).

3.5. Effect of GR15 peptide on the disruption of cell cycle

The further characterize the anti-cancer property of GR15, cell cycle analysis was carried out. Based on the outcome in the previous assays, two concentrations (25 and 45 μM) of GR15 were chosen for the cell cycle analysis. Results revealed that 25 μM and 45 μM GR15 challenge led to difference in the cell populations in the SUB G1 and G0/G1 phases than the untreated control. How-

ever, this difference is prominent in 45 μM than in 25 μM GR15 challenge. The total percentage of the cell population in its various stages was calculated (Figs. 7A and 7B). This observation shows that GR15 significantly altered the cell-cycle stages than the control.

3.6. Effect of GR15 on the mRNA expression of anti-cancer genes

The GR15 peptide at 45 μM showed a half-fold increase in Bcl-2, threefold increase in BAX, fourfold increase in Caspase-3 and above fivefold increase in Caspase-9 expressions compared to the control (Fig. 8). Data were shown after normalized with the GAPDH (housekeeping gene).

3.7. Docking study

Molecular docking was performed to evaluate the receptor-ligand binding ability between GR15 and the select anti-cancer molecules. Results showed that the binding energy for BAX is -166.8637 kcal/mol, Bcl-2 is -191.2777 kcal/mol, Caspase-3 is -164.7637 kcal/mol, and Caspase-9 is -167.8727 kcal/mol. A good number of amino acid interactions on the H bond of GR15 (E-Suppl. Table 1) was visualized in the discovery studio software (Fig. 9), which establishes the *in-vitro* outcome, *i.e.*, the anti-cancer nature of GR15.

4. Discussion

Our previous report shows that the peptide, GR15, derived from S-adenosylmethionine synthase of *A. platensis* has antioxidant effect, wherein the H_2O_2 -induced oxidative stress on *in-vitro* MDCK cells and *in-vivo*, zebrafish larval models were utilized (Velayutham et al., 2021). Recent studies report that antioxidant molecules could also have anti-cancer effect as well (Ovando et al., 2018). The antioxidant peptide YT12 derived from the peroxiredoxin protein of sulfur-deprived *A. platensis* showed significant anti-cancer effect against colon cancer cells, HT-29 (Sannasimuthu et al., 2020). Based on these observations, this study investigated the anti-cancer effect of GR15 in breast cancer cells. An advantage of GR15 is that this peptide is non-toxic and it reduces the ROS level in MDCK cells (Velayutham et al., 2021).

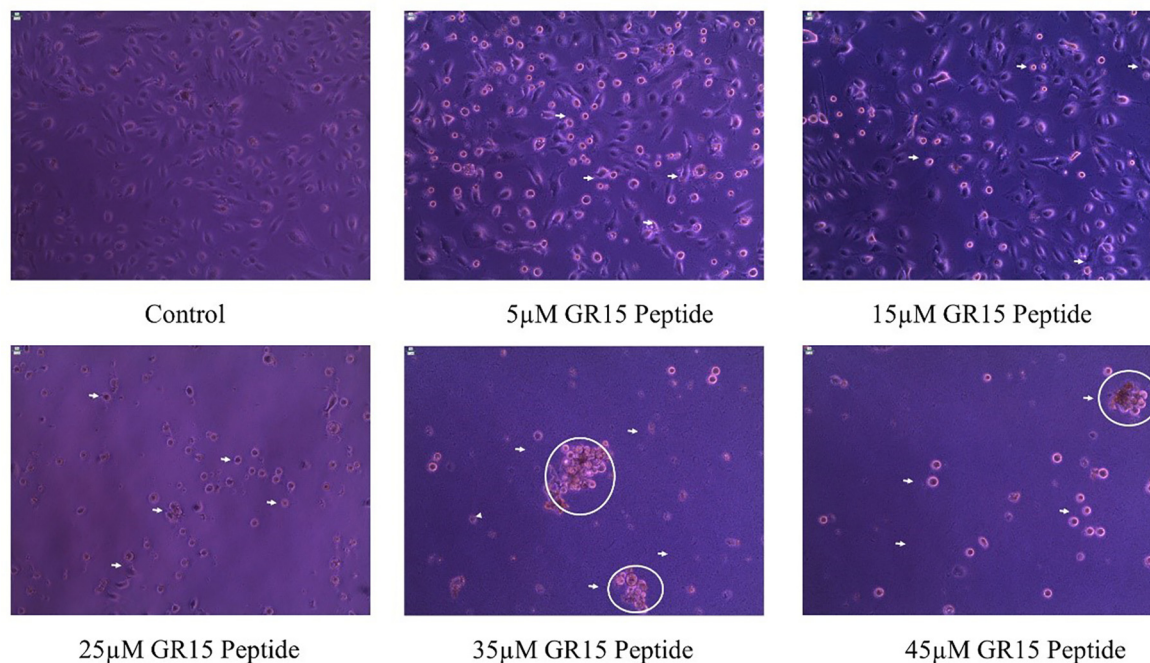


Fig. 3. Influence of GR15 peptide alteration on cellular morphology in MCF-7 (Breast cancer cells). The peptide was treated with five concentrations for 24 h, and the results were compared with the untreated control group.

In this study, the MTT assay results showed significant inhibition in the proliferation of breast cancer cells, which is a dose-dependent effect. [Zarandi et al. \(2019\)](#), has stated that the bioactive peptide ICD-85, less than 3000 Da showed significant anti-proliferative properties on cancer cells. Similarly, GR15, whose molecular mass is 1490 Da or less than 3000 Da has anti-proliferative effect. [Chiangjong et al. \(2020\)](#) reported the importance of amino acid function to realize the anti-cancer nature of the peptide. In line with this report, the amino acid sequence of GR15 is: Gly, Lys, Pro, Thr, Val, Asp, and Arg, which is responsible for the peptide's anti-cancer nature. Trypan blue exclusion assay validated the anti-proliferative nature of GR15 by differentiating the live and dead cells in this study. As noticed in the MTT assay, in this assay also, both live and dead cells were observed, and their population percentage was calculated. Our results corroborate with the observation of [Dasiram et al. \(2017\)](#) who explored the anti-cancer nature of bioactive compounds from curcumin and demonstrated such effect on the colon adenocarcinoma cells.

Lactate dehydrogenase is the cytosolic enzyme released into the culture medium due to the loss of cell membrane integrity or damage. The GR15-exposed cells showed a dose-dependent increase in the total LDH level compared to the untreated control. This observation suggests that GR15 is involved in the cell membrane disruption. Recent studies have reported ([Chiangjong et al., 2020](#)) that the amino acids Arg and Lys are positively charged and that these residues damage the cell membrane integrity to penetrate the cell, which leads to cytotoxicity in cancer cells. It is possible that GR15 targets the cell membrane, as its sequence has Arg and Lys, which eventually leads to loss of cell membrane integrity and the associated morphological changes in cells. Similar findings were reported in a peptide isolated from *Grapsus albacarinus* for antitumor activity against MCF-7 cells ([Emadi Shaibani et al., 2021](#)). The cytomorphology analysis reveals that the GR15-exposed cells undergo apoptosis. The AO/PI fluorescent dye-based assay was performed to understand the type of cell death and/or stages of apoptosis, induced by GR15. All the five concentrations of GR15 treatment

increased a significant number of early and late apoptotic cells. Likewise, a bio-active molecule named, Nymphyol is reported to induce apoptotic cell death in MCF-7 cells ([Al-Harbi et al., 2020](#)).

GR15 significantly reduced the concentration of ROS in MDCK cells under H_2O_2 induced oxidative stress ([Velayutham et al., 2021](#)). In breast cancer cells, an imbalance in the ROS concentration led to apoptosis, while GR15 exposure for 24 h showed a dose-dependent reduction in ROS level. Similar to our observation, an antioxidant peptide, YT12, showed significant ROS reduction in HT-29 cancer cells ([Sannasimuthu et al., 2020](#)). One of the mechanisms by which anti-cancer activity has been achieved is through mitochondria-mediated apoptosis. GR15 challenge showed a dose-dependent elevation in ROS and apoptotic activity. The imbalanced state of ROS condition leads to mitochondrial damage. A similar result was reported by [Siddiqui et al. \(2013\)](#), that functionalized multiwalled carbon nanotubes showed dose-dependent activity on the mitochondrial membrane potential. Based on this report, it is possible for GR15 to damage the mitochondria in MCF-7 cells. Cell cycle analysis in breast cancer cells showed that GR15 exposure led to accumulation of cells or cell cycle arrest in SUB G1 and G0/G1 phases. Our observations correlated with a peptide derived from the mucus protein of *Anabas testudineus* showed cell cycle arrest on G1 phases of MCF7 and MDA-MB-231 cells ([Najm et al., 2021](#)). GR15 significantly altered the expression of different genes associated with apoptotic signaling cascade. GR15 induced the caspase-mediated apoptotic pathway through caspase-3 and caspase-9 upregulation. An earlier study on RF13 peptides is in line with the present observation, wherein RF13 showed anti-cancer activity by regulating the caspase-mediated apoptosis ([Velayutham et al., 2022](#)). Our molecular docking analysis validated the *in-vitro* results, as has been evaluated previously ([Lee et al., 2019](#)). GR15 shows significant binding score with the anti-cancer protein molecules; this approach has been supported by a previous study which showed that the peptide RF13 significantly binds with the anti-cancer proteins ([Velayutham et al., 2022](#)).

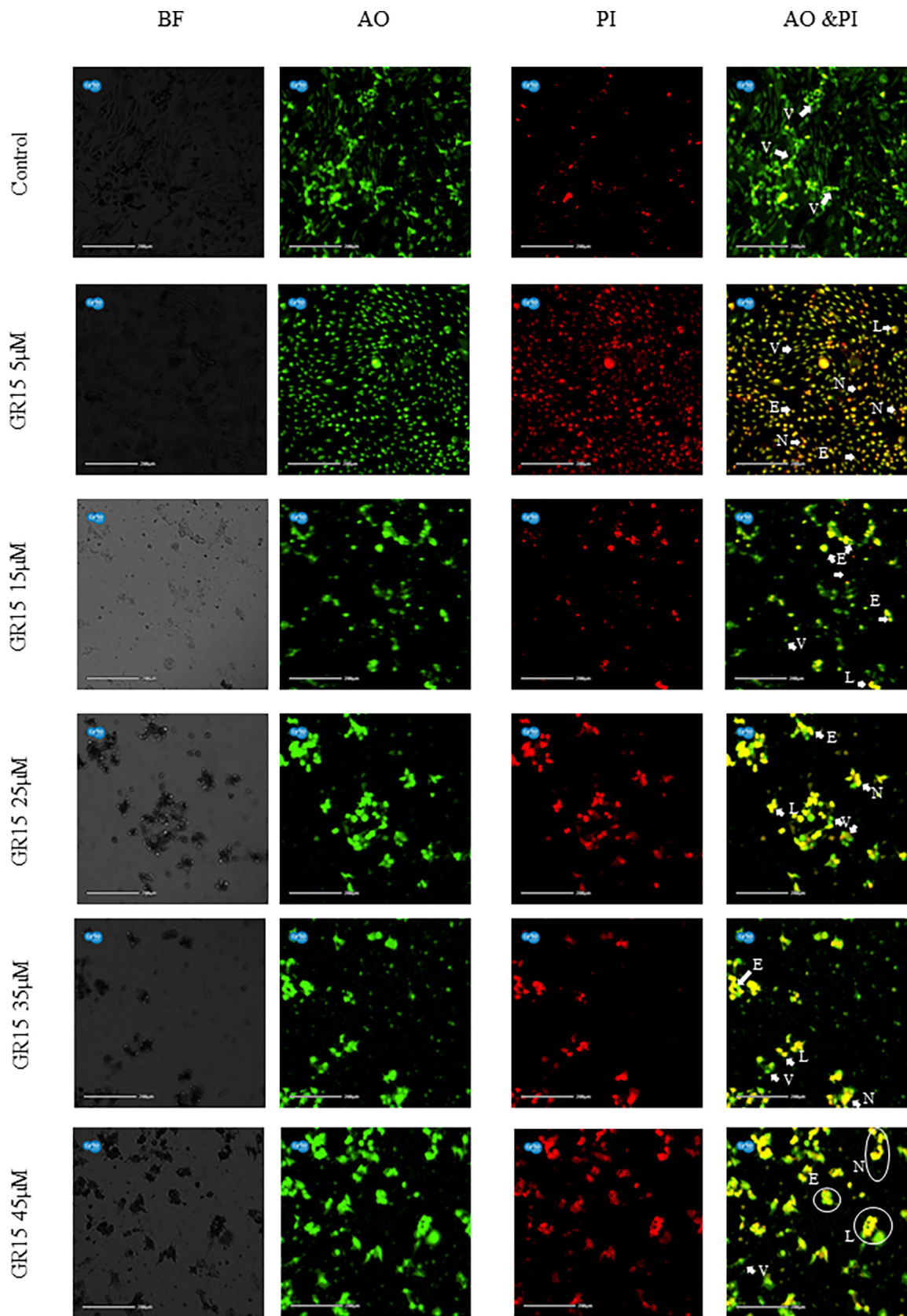


Fig. 4. Photomicrographs represent the apoptotic staining of MCF-7 cells by AO/PI. The MCF-7 cells were treated with five different concentrations of GR15 peptide. The apoptotic stage in control (untreated) is indicated in white arrows and circles. BF – Bright Field, AO – Acridine orange staining, PI – Propidium iodide staining, and AO & PI – merged images of both the staining. Viable cells were observed in green fluorescent in control, and early and late apoptosis was observed as yellow and reddish-orange in colour—V-Viable cells, E – Early apoptotic cells, L-Late apoptotic cells, and N – Necrotic cells.

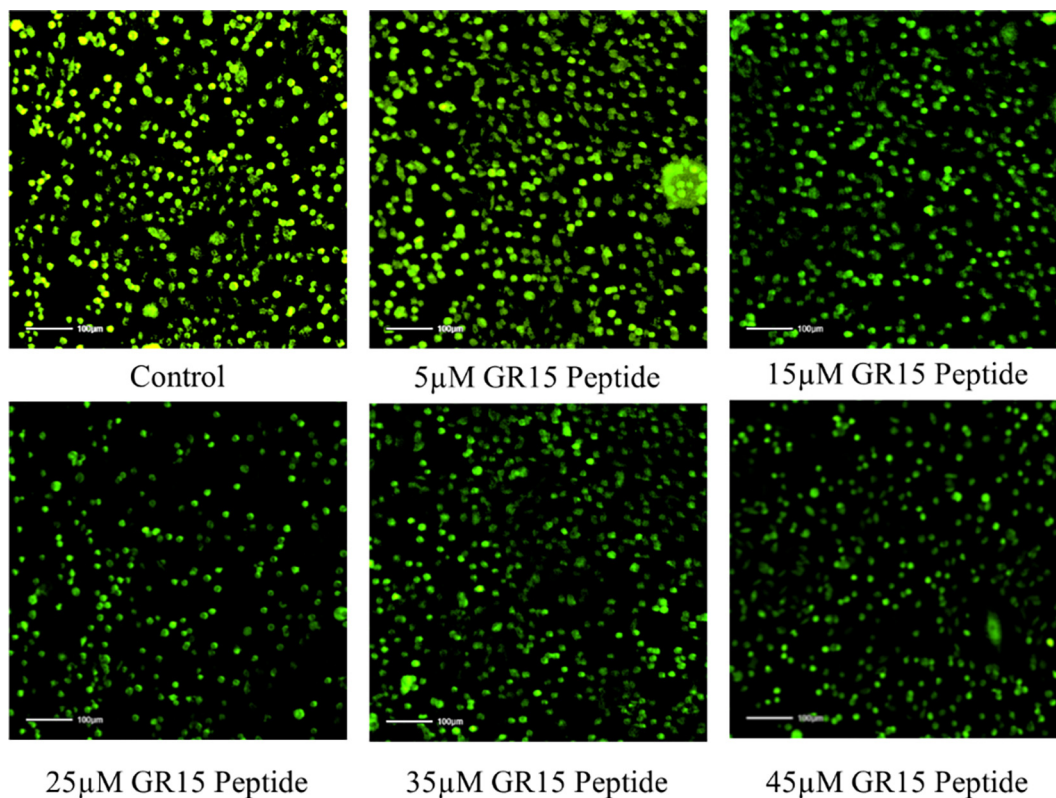


Fig. 5. Intracellular ROS measurement of GR15 peptide treated MCF-7. The peptide treatment group showed a dose-dependent decrease in ROS level compared to the control group.

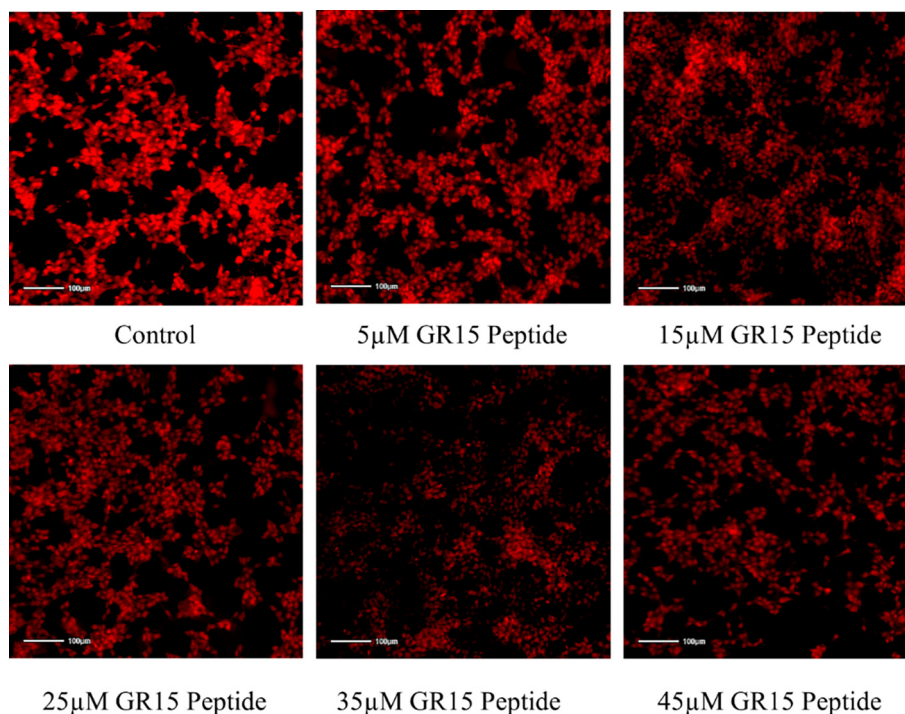


Fig. 6. Measurement of mitochondria membrane potential activity by rhodamine 123, the peptide treatment group showed dose-dependent activity on MCF-7 cells compared to the control (untreated) group.

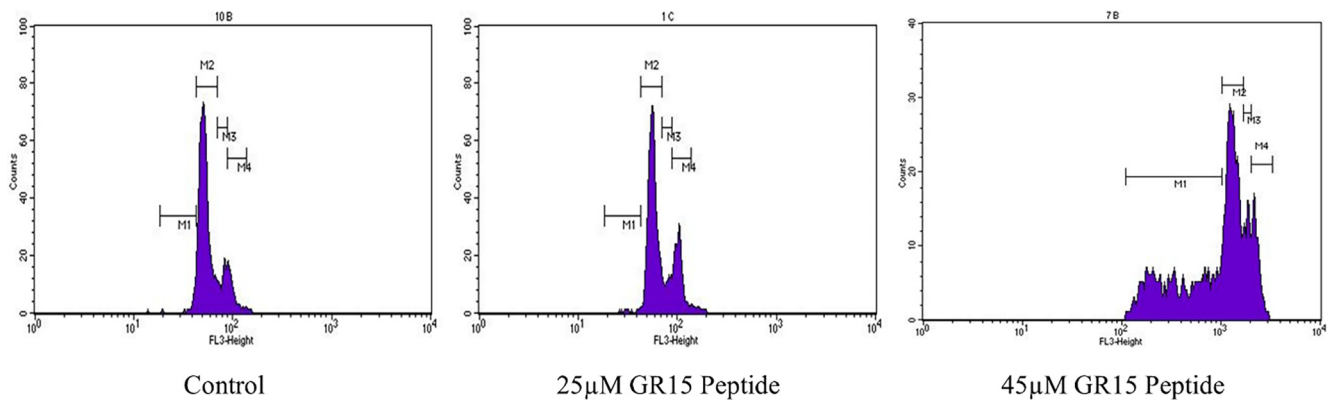


Fig. 7A. Fluorescence-activated cell sorting (FACS) analysis through PI staining on MCF-7 cells treated with two different concentrations of GR15 (25 and 45 µM) for 24 h and control (untreated).

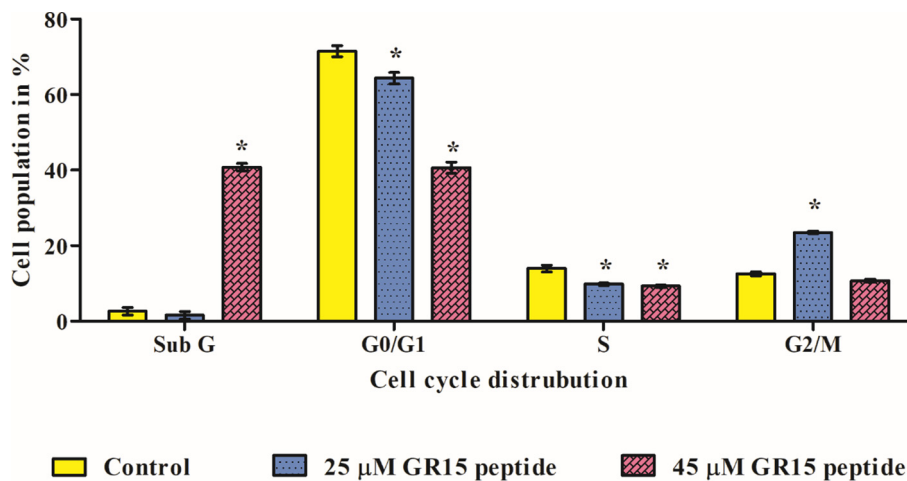


Fig. 7B. Fluorescence-activated cell sorting (FACS) analysis through PI staining on MCF-7 cells, calculating the population percentage of cell cycle stages. The data on the cells treated with GR15 was compared with the untreated control and showed statistical significance at $p < 0.05$, indicated by the asterisk (*). The data provided in mean \pm SD of three independent experiments.

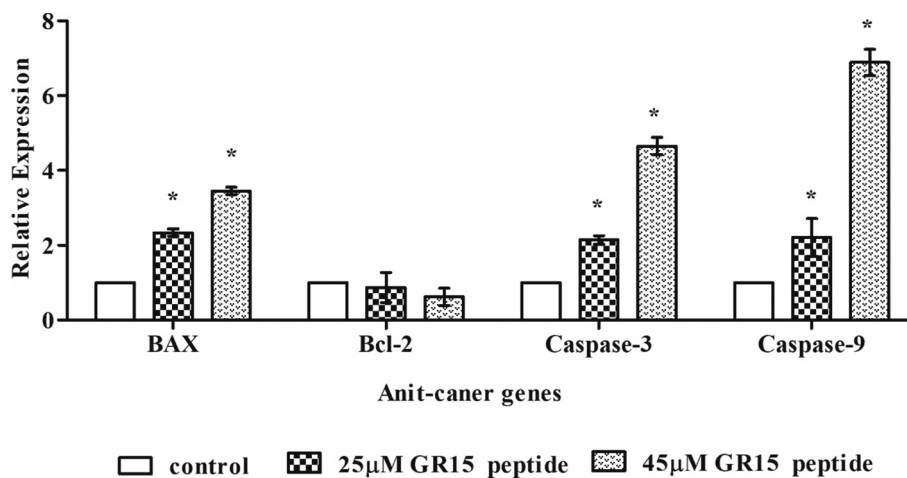


Fig. 8. Gene expression analysis of GR15 peptide effect on MCF-7 cells. Genes expression data were normalised with the housekeeping molecule GAPDH. The data presented in mean \pm standard deviation (SD) of three independent experiments. The asterisk (*) denotes the significance level at $p < 0.05$ compared to the control.

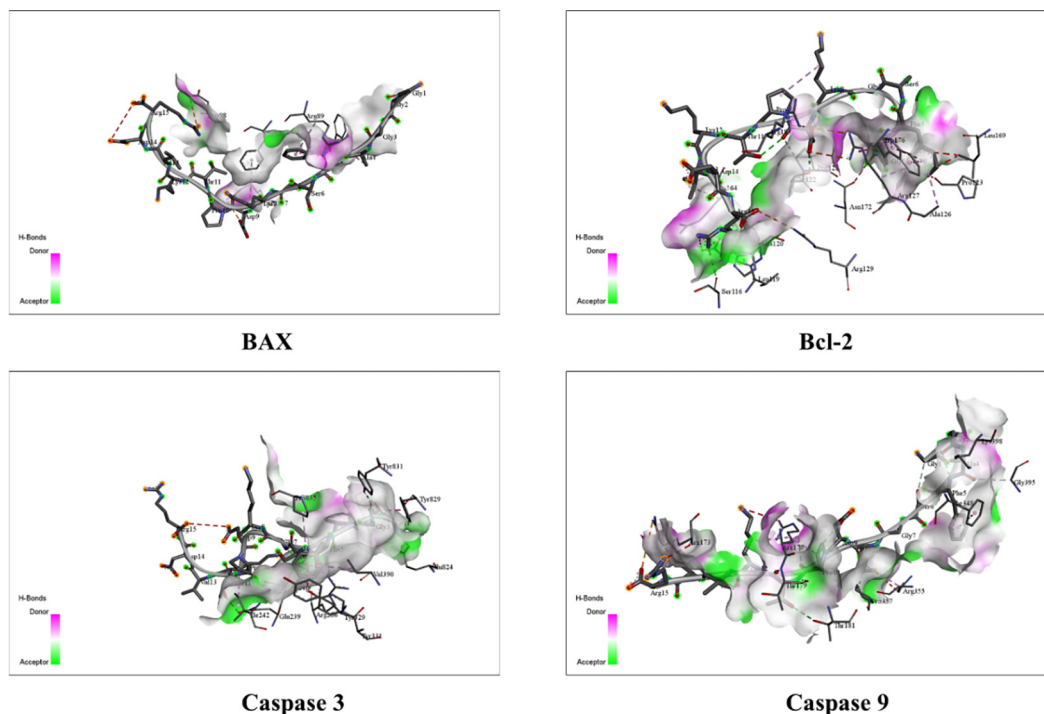


Fig. 9. Molecular docking of GR15 with anticancer receptor to understand the amino acid interaction between the peptide and available anticancer proteins. Docking was performed using the HEPDOCK web server. The data were visualised in discovery studio software.

5. Conclusion

We propose that the antioxidant peptide GR15, derived from the *S*-adenosylmethionine synthase protein of *A. platensis*, elicits anti-cancer effect on breast cancer cells. However, *in-vivo* and clinical studies are needed before the molecule can be utilized as a drug for anti-cancer therapeutic use to understand the pharmacodynamic aspect and drug delivery performance of GR15 in an *in-vivo* model, which is a future concern of this research.

CRedit authorship contribution statement

Manikandan Velayutham: Conceptualization, Methodology, Data curation, Writing – original draft. **B. Haridevamuthu:** . **Mohamed Farouk Elsadek:** Methodology, Resources. **Humaira Rizwana:** Methodology, Resources. **Annie Juliet:** Methodology, Resources. **Kanchana M. Karuppiah:** Conceptualization, Methodology, Resources, Supervision. **Jesu Arockiaraj:** Conceptualization, Methodology, Resources, Supervision.

Declaration of Competing Interest

The authors declare that they have no known competing financial interests or personal relationships that could have appeared to influence the work reported in this paper.

Acknowledgement

The authors extend their appreciation to the Researchers Supporting Project Number (RSP-2021/349), King Saud University, Riyadh, Saudi Arabia.

Appendix A. Supplementary data

Supplementary data to this article can be found online at <https://doi.org/10.1016/j.jksus.2022.102354>.

References

- Ahamed, M., Alhadlaq, H., 2014. Nickel nanoparticle-induced dose-dependent cytotoxicity in human breast carcinoma MCF-7 cells. *Onco. Targets. Ther.* 269. <https://doi.org/10.2147/OTT.S58044>.
- Al-Harbi, L.N., Subash-Babu, P., Binobeat, M.A., Alhussain, M.H., Alsedairy, S.A., Aloud, A.A., Alshatwi, A.A., 2020. Potential metabolite nymphaol isolated from water lily (*Nymphaea stellata*) flower inhibits MCF-7 human breast cancer cell growth via upregulation of CDKN2A, PRB2, P53 and downregulation of PCNA mRNA expressions. *Metabolites* 10, 1–14. <https://doi.org/10.3390/metabo10070280>.
- Al-Qubaisi, M., Rozita, R., Yeap, S.K., Omar, A.R., Ali, A.M., Alitheen, N.B., 2011. Selective cytotoxicity of goniothalamin against hepatoblastoma HepG2 cells. *Molecules* 16, 2944–2959. <https://doi.org/10.3390/molecules16042944>.
- Anastasiadi, Z., Lianos, G.D., Ignatiadou, E., Harissis, H.V., Mitsis, M., 2017. Breast cancer in young women: an overview. *Updates Surg.* 69, 313–317. <https://doi.org/10.1007/s13304-017-0424-1>.
- Anjum, F., Razvi, N., Masood, M.A., 2017. Breast cancer therapy: a mini review. *MOJ Drug Des. Dev. Ther.* 1, 35–38. <https://doi.org/10.15406/mojddt.2017.01.00006>.
- Bray, F., Laversanne, M., Weiderpass, E., Soerjomataram, I., 2021. The ever-increasing importance of cancer as a leading cause of premature death worldwide. *Cancer* 127, 3029–3030. <https://doi.org/10.1002/cncr.33587>.
- Çakır, B., Okuyan, B., Şener, G., Tunali-Akbay, T., 2021. Investigation of beta-lactoglobulin derived bioactive peptides against SARS-CoV-2 (COVID-19): *In silico analysis*. *Eur. J. Pharmacol.* 891, 173781.
- Chen, Z., Li, W., Santhanam, R.K., Wang, C., Gao, X., Chen, Y., Wang, C., Xu, L., Chen, H., 2019. Bioactive peptide with antioxidant and anticancer activities from black soybean [*Glycine max* (L.) Merr.] byproduct: isolation, identification and molecular docking study. *Eur. Food Res. Technol.* 245, 677–689. <https://doi.org/10.1007/s00217-018-3190-5>.
- Chiangjong, W., Chutipongtanate, S., Hongeng, S., 2020. Anticancer peptide: physicochemical property, functional aspect and trend in clinical application (Review). *Int. J. Oncol.* 57, 678–696. <https://doi.org/10.3892/ijo.2020.5099>.
- Chiu, H.-W., Yeh, Y.-L., Wang, Y.-C., Huang, W.-J., Ho, S.-Y., Lin, P., Wang, Y.-J., 2016. Combination of the novel histone deacetylase inhibitor YCW1 and radiation induces autophagic cell death through the downregulation of BNIP3 in triple-negative breast cancer cells *in vitro* and in an orthotopic mouse model. *Mol. Cancer* 15, 46. <https://doi.org/10.1186/s12943-016-0531-5>.

- Correia, A.S., Gärtner, F., Vale, N., 2021. Drug combination and repurposing for cancer therapy: the example of breast cancer. *Heliyon* 7 (1). <https://doi.org/10.1016/j.heliyon.2021.e05948>.
- Crupi, R., Palma, E., Siracusa, R., Fusco, R., Gugliandolo, E., Cordaro, M., Impellizzeri, D., De Caro, C., Calzetta, L., Cuzzocrea, S., Di Paola, R., 2020. Protective Effect of Hydroxytyrosol Against Oxidative Stress Induced by the Ochratoxin in Kidney Cells: in vitro and in vivo Study. *Front. Vet. Sci.* 7, 1–13. <https://doi.org/10.3389/fvets.2020.00136>.
- Emadi Shaibani, M., Heidari, B., Khodabandeh, S., Shahangian, S.S., 2021. Production and Fractionation of Rocky Shore Crab (*Grapsus albacarinos*) Protein Hydrolysate by Ultrafiltration Membrane: Assessment of Antioxidant and Cytotoxic Activities. *J. Aquat. Food Prod. Technol.* 30, 339–352. <https://doi.org/10.1080/10498850.2021.1882631>.
- Fleischauer, A.T., Simonsen, N., Arab, L., 2003. Antioxidant supplements and risk of breast cancer recurrence and breast cancer-related mortality among postmenopausal women. *Nutr. Cancer* 46, 15–22. https://doi.org/10.1207/S15327914NC4601_02.
- Guzmán, F., Wong, G., Román, T., Cárdenas, C., Álvarez, C., Schmitt, P., Albericio, F., Rojas, V., 2019. Identification of Antimicrobial Peptides from the Microalgae *Tetraselmis suecica* (Kylin) Butcher and Bactericidal Activity Improvement. *Mar. Drugs* 17, 1–19. <https://doi.org/10.3390/md17080453>.
- Kurrikoff, K., Aphkhasava, D., Langel, Ü., 2019. The future of peptides in cancer treatment. *Curr. Opin. Pharmacol.* 47, 27–32. <https://doi.org/10.1016/j.coph.2019.01.008>.
- Lee, A.C.L., Harris, J.L., Khanna, K.K., Hong, J.H., 2019. A comprehensive review on current advances in peptide drug development and design. *Int. J. Mol. Sci.* 20, 1–21. <https://doi.org/10.3390/ijms20102383>.
- Mikaelian, A.G., Traboulay, E., Zhang, X.M., Yeritsyan, E., Pedersen, P.L., Ko, Y.H., Matalka, K.Z., 2020. Pleiotropic anticancer properties of scorpion venom peptides: *Rhopalurus princeps* venom as an anticancer agent. *Drug Des. Devel. Ther.* 14, 881–893. <https://doi.org/10.2147/DDDT.S231008>.
- Najm, A.A.K., Azfaralariff, A., Dyari, H.R.E., Othman, B.A., Shahid, M., Khalili, N., Law, D., Syed Alwi, S.S., Fazry, S., 2021. Anti-breast cancer synthetic peptides derived from the *Anabas testudineus* skin mucus fractions. *Sci. Rep.* 11, 1–20. <https://doi.org/10.1038/s41598-021-02007-6>.
- Ovando, C.A., de Carvalho, J.C., de Melo, V., Pereira, G., Jacques, P., Soccol, V.T., Soccol, C.R., 2018. Functional properties and health benefits of bioactive peptides derived from *Spirulina*: A review. *Food Rev. Int.* 34, 34–51. <https://doi.org/10.1080/87559129.2016.1210632>.
- Prabha, N., Sannasimuthu, A., Kumaresan, V., Elumalai, P., Arockiaraj, J., 2020. Intensifying the Anticancer Potential of Cationic Peptide Derived from Serine Threonine Protein Kinase of Teleost by Tagging with Oligo Tryptophan. *Int. J. Pept. Res. Ther.* 26, 75–83. <https://doi.org/10.1007/s10989-019-09817-3>.
- Sannasimuthu, A., Ramani, M., Pasupuleti, M., Saraswathi, N.T., Arasu, M.V., Al-Dhabi, N.A., Arshad, A., Mala, K., Arockiaraj, J., 2020. Peroxiredoxin of *Arthrospira platensis* derived short molecule YT12 influences antioxidant and anticancer activity. *Cell Biol. Int.* 44, 2231–2242. <https://doi.org/10.1002/cbin.11431>.
- Siddiqui, M.A., Alhadlaq, H.A., Ahmad, J., Al-Khedhairi, A.A., Musarrat, J., Ahamed, M., Pant, A.B., 2013. Copper Oxide Nanoparticles Induced Mitochondria Mediated Apoptosis in Human Hepatocarcinoma Cells. *PLoS One* 8 (8). <https://doi.org/10.1371/journal.pone.0069534>.
- Silva, M.R.O.B. da, M. da Silva, G., Silva, A.L.F. da, Lima, L.R.A. de, Bezerra, R.P., Marques, D. de A. V., 2021. Bioactive Compounds of *Arthrospira* spp. (*Spirulina*) with Potential Anticancer Activities: A Systematic Review. *ACS Chem. Biol.* 16, 2057–2067. doi: 10.1021/acscchembio.1c00568.
- Sung, H., Ferlay, J., Siegel, R.L., Laversanne, M., Soerjomataram, I., Jemal, A., Bray, F., 2021. Global Cancer Statistics 2020: GLOBOCAN Estimates of Incidence and Mortality Worldwide for 36 Cancers in 185 Countries. *CA. Cancer J. Clin.* 71, 209–249. <https://doi.org/10.3322/caac.21660>.
- Velayutham, M., Guru, A., Arasu, M.V., Al-Dhabi, N.A., Choi, K.C., Elumalai, P., Hari Krishnan, R., Arshad, A., Arockiaraj, J., 2021. GR15 peptide of S-adenosylmethionine synthase (SAMe) from *Arthrospira platensis* demonstrated antioxidant mechanism against H2O2 induced oxidative stress in in-vitro MDCK cells and in-vivo zebrafish larvae model. *J. Biotechnol.* 342, 79–91. <https://doi.org/10.1016/j.jbiotec.2021.10.010>.
- Velayutham, M., Guru, A., Gatasheh, M.K., Hatamleh, A.A., Juliet, A., Arockiaraj, J., 2022a. Molecular docking of SA11, RF13 and D14 peptides from vacuolar protein sorting associated protein 26B against cancer proteins and in vitro investigation of its anticancer potency in Hep-2 cells. *Int. J. Pept. Res. Ther.* 28, 87. <https://doi.org/10.1007/s10989-022-10395-0>.
- Velayutham, M., Haridevamuthu, B., Priya, P.S., Ganesh, M.R., Arockiaraj, Jesu, 2022b. Serine O-acetyltransferase derived NV14 peptide reduces cytotoxicity in H 2 O 2 induced MDCK cells and inhibits MCF-7 cell proliferation through caspase gene expression. *Mol. Biol. Rep.* 1–11. <https://doi.org/10.1007/s11033-022-07746-x>.
- Velayutham, M., Sarkar, P., Rajakrishnan, R., Kuppusamy, P., Juliet, A., Arockiaraj, J., 2022c. Antiproliferation of MP12 derived from a fungus, *Aphanomyces invadans* virulence factor, cysteine-rich trypsin inhibitor on human laryngeal epithelial cells, and in vivo zebrafish embryo model. *Toxicol.* 210, 100–108. <https://doi.org/10.1016/j.toxicol.2022.02.019>.
- Zarandi, P.K., Mirakabadi, A.Z., Sotoodehnejadnematalahi, F., 2019. Cytotoxic and anticancer effects of ICD-85 (Venom derived peptides) in human breast adenocarcinoma and normal human dermal fibroblasts. *Iran. J. Pharm. Res.* 18, 232–240. <https://doi.org/10.22037/ijpr.2019.2341>.
- Zarei, M., Shivanandappa, T., Zarei, M., 2020. Natural bioactive 4-Hydroxyisophthalic acid (4-HIPA) exhibited antiproliferative potential by upregulating apoptotic markers in in vitro and in vivo cancer models. *Mol. Biol. Rep.* 47, 5343–5353. <https://doi.org/10.1007/s11033-020-05617-x>.